Optically Active Transition Metal Complexes. 109.[1] Novel (η^6-Benzene)ruthenium Complexes with a Chiral Pyrrolecarbaldiminato Chelate Ligand: Synthesis, Crystal Structures, Properties, and Stereochemistry at the Ruthenium Atom

Henri Brunner* and Ralf Oeschey

Institut für Anorganische Chemie der Universität Regensburg, D-93053 Regensburg, Germany

Bernd Nuber

Anorganisch-Chemisches Institut der Universität Heidelberg, D-69120 Heidelberg, Germany

Received March 22, 1996[⊗]

The reaction of $[(\eta^6\text{-}C_6H_6)RuCl_2]_2$ with the sodium salt of (+)-(*S*)-*N*-(1-phenylethyl)-pyrrolecarbaldimine (HLL*) in CH_2Cl_2 yielded a mixture of the two diastereomers (S_{Ru},S_C)- and (R_{Ru},S_C)-$[(\eta^6\text{-}C_6H_6)Ru(LL^*)Cl]$ (**1a**,**b**) in a ratio of 68:32. The chloride ligand in **1a**,**b** was replaced in methanol by triphenylphosphane to give the two diastereomers (S_{Ru},S_C)- and (R_{Ru},S_C)-$[(\eta^6\text{-}C_6H_6)Ru(LL^*)(PPh_3)]PF_6$ (**2a,b**). According to variable-temperature ^{1}H NMR studies the formation of configurationally labile solvate intermediates has to be assumed in the reaction of the chloro complexes **1a**,**b** with triphenylphosphane in the solvent methanol. In contrast to the diastereomers **1a**,**b**, the ruthenium configuration in the phosphane complexes **2a**,**b** is configurationally stable at room temperature. The diastereomers **2a**,**b** were separated by crystallization. The crystal structures of (S_{Ru},S_C)-**1a**, (S_{Ru},S_C)-**2a**, and (R_{Ru},S_C)-**2b** were determined by X-ray analysis. The epimerization of **2b** at 85 °C in nitromethane-d_3 gave a 93.5:6.5 equilibrium mixture of **2a** and **2b** ($\tau_{1/2}$ (min) = 58.2 ± 0.4). Conformational analyses showed that two main factors govern the orientation of the 1-phenylethyl group relative to the $[(\eta^6\text{-}C_6H_6)Ru(LL^*)X]$ moiety (X = Cl, PPh_3): (i) the face-on orientation of the phenyl substituent with respect to the π-bonded benzene ligand and (ii) the orientation of the hydrogen substituent toward the unidentate ligand L.

Introduction

Optically active transition-metal complexes have proven their usefulness in stoichiometric stereoselective synthesis[2,3] and enantioselective catalysis.[4] Because of the potential application in catalysis, ruthenium complexes are of particular interest. Following the first resolution of a ruthenium complex chiral at the Ru atom,[5] detailed studies concerning the stereochemistry of ruthenium complexes were carried out.[6] *In situ* catalysts consisting of (arene)ruthenium complexes and chiral chelating Schiff base ligands gave moderate enantiomeric excesses (ee's) in the hydrogen transfer reduction of alkyl aryl ketones with 2-propanol.[7] With dimeric (arene)ruthenium procatalysts and (*S*)- or (*R*)-BINAP cocatalysts Noyori and Takaya obtained extremely high optical inductions in the hydrogenation of both prochiral alkenes and ketones.[8,9] Use of water-soluble, sulfonated BINAP ligands allowed biphasic reaction control.[10]

Recently, we reported our results on the optically active (arene)ruthenium complexes $[(\eta^6\text{-Ar})Ru(LL^*)Cl]$ and $[(\eta^6\text{-Ar})Ru(LL^*)L]PF_6$ (Ar = *p*-cymene, benzene; LL* = anion of (*S*)-*N*-(1-phenylethyl)salicylaldimine; L = triphenylphosphane, 2- and 4-methylpyridine),[1,11−14] correcting publications[15−17] in which a high stability had been ascribed to the stereogenic ruthenium center. We could demonstrate that epimerization at the ruthenium atom was fast in these compounds, which contain the N,O donor set of the chiral salicylaldiminato ligand, and substitution reactions proceeded without retention of the metal configuration.

In the present paper we describe the synthesis and characterization of the (benzene)ruthenium complexes $[(\eta^6\text{-}C_6H_6)Ru(LL^*)Cl]$ and $[(\eta^6\text{-}C_6H_6)Ru(LL^*)(PPh_3)]PF_6$,

[⊗] Abstract published in *Advance ACS Abstracts,* July 15, 1996.

(1) Part 108: Brunner, H.; Oeschey, R.; Nuber, B. *J. Organomet. Chem.* **1996**, *518*, 47.
(2) Blackburn, K.; Davies, S. G.; Whittaker, M. In *Chemical Bonds-Better Ways to Make Them and to Break Them*; Bernal, I., Ed.; Elsevier: New York, 1989; p 141.
(3) Stark, G. A.; Dewey, M. A.; Richter-Addo, G. B.; Knight, D. A.; Arif, A. M.; Gladysz, J. A. In *Stereoselective Reactions of Metal-Activated Molecules*; Werner, H., Sundermeyer, J., Eds.; Vieweg: Stuttgart, Germany, 1995; p 51.
(4) Brunner, H.; Zettlmeier, W. *Handbook of Enantioselective Catalysis*; VCH: Weinheim, Germany, 1993.
(5) Brunner, H.; Gastinger, R. G. *J. Chem. Soc., Chem. Commun.* **1977**, 488.
(6) Consiglio, G.; Morandini, F. *Chem. Rev.* **1987**, *87*, 761.
(7) Krasik, P.; Alper, H. *Tetrahedron* **1994**, *50*, 4347.
(8) Ohta, T.; Takaya, H.; Kitamura, M.; Nagai, K.; Noyori, R. *J. Org. Chem.* **1987**, *52*, 3174.
(9) Mashima, K.; Kusano, K.; Sato, N.; Matsumura, Y.; Nozaki, K.; Kumobayashi, H.; Sayo, Y.; Hori, Y.; Ishizaki, T.; Akutagawa, S.; Takaya, H. *J. Org. Chem.* **1994**, *59*, 3064.
(10) Wan, K. T.; Davis, M. E. *Nature* **1994**, *370*, 449.
(11) Oeschey, R. Ph.D. Thesis, University of Regensburg, 1995.
(12) Brunner, H.; Oeschey, R.; Nuber, B. *Angew. Chem.* **1994**, *106*, 941; *Angew. Chem., Int. Ed. Engl.* **1994**, *33*, 866.
(13) Brunner, H.; Oeschey, R.; Nuber, B. *Inorg. Chem.* **1995**, *34*, 3349.
(14) Brunner, H.; Oeschey, R.; Nuber, B. *J. Chem. Soc., Dalton Trans.* **1996**, 1499.
(15) Mandal, S. K.; Chakravarty, A. R. *J. Organomet. Chem.* **1991**, *417*, C59.
(16) Mandal, S. K.; Chakravarty, A. R. *J. Chem. Soc., Dalton Trans.* **1992**, 1627.
(17) Mandal, S. K.; Chakravarty, A. R. *Inorg. Chem.* **1993**, *32*, 3851.

S0276-7333(96)00215-4 CCC: $12.00

Table 1. ^{1}H NMR Data of the Complexes (S_{Ru},S_C)- and (R_{Ru},S_C)-[(η^6-C_6H_6)Ru(LL*)Cl] (1a,b) and (S_{Ru},S_C)- and (R_{Ru},S_C)-[(η^6-C_6H_6)Ru(LL*)(PPh$_3$)]PF$_6$ (2a,b)[a]

complex	LL*[b]	η^6-C_6H_6	L′ [b]
1a,**b**[c]	1.75/1.98 (3 H, d, $^3J_{HH}$ 6.9/6.8, CHCH_3) 5.61/5.08 (1 H, q, $^3J_{HH}$ 6.9/6.8, CHCH$_3$) 6.37/6.34 (1 H, dd, $^3J_{HH}$ 3.9, $^3J_{HH}$ 1.8, H^4 Pyr)[d] 6.80/6.74 (1 H, dd, $^3J_{HH}$ 3.9, $^4J_{HH}$ 1.1, H^3 Pyr) 7.28 (1 H, s, CHCl$_3$) 7.39−7.49 (5 H, m, Ph−Pyr) 7.57/7.52 (1 H, br s, H^5 Pyr) 7.87/7.76 (1 H, br d, $^4J_{HH}$ 0.4/0.7, N=CH)		
2a[e]	1.05 (3 H, d, $^3J_{HH}$ 7.0, CHCH_3) 5.30 [1 H, q, $^3J_{HH}$ 7.0, CHCH$_3$] 6.17 [1 H, dd, $^3J_{HH}$ 3.9, H^4 Pyr][f] 6.80 (1 H, ddd, $^3J_{HH}$ 3.9, $^4J_{HH}$ 1.1, $^5J_{HP}$ 1.5, H^3 Pyr) 7.35 (1 H, br m, H^5 Pyr) 7.42−7.47 (1 H, m, H$_{para}$ Ph) 7.50−7.53 (4 H, m, H$_{meta}$ + H$_{ortho}$ Ph)[g] 7.78 (1 H, d, $^4J_{HP}$ 2.6, N=CH)	5.68 (d, $^3J_{HP}$ 0.7)	7.21 (6 H, AA′ part of a AA′BB′C system, $^3J_{HH}$ 7.4, $^3J_{HP}$ 7.2, $^4J_{HH}$ 1.3, H_{ortho}-PPh$_3$) 7.50−7.53 (6 H, BB′ part of a AA′BB′C system, m, H$_{meta}$ PPh$_3$)[g] 7.60 (3 H, C part of a AA′BB′C system, $^3J_{HH}$ 7.4, $^4J_{HH}$ 1.3, H$_{para}$ PPh$_3$)
2b[h]	1.87 (3 H, d, $^3J_{HH}$ 6.8, CHCH_3) 5.46 (1 H, q, $^3J_{HH}$ 6.8, CHCH$_3$) 6.11 [1 H, dd, $^3J_{HH}$ 3.9, $^3J_{HH}$ 1.8, H^4 Pyr] 6.36 (1 H, m, H^3 Pyr)[f] 7.14 (2 H, m, H$_{ortho}$ Ph) 7.21 (2 H, m, H$_{meta}$ Ph)[i] 7.33 (1 H, m, H$_{para}$ Ph) 7.58−7.70 (1 H, m, H^5 Pyr)[g] 8.00 (d, $^4J_{HP}$ 2.6, N=CH)	6.37[f]	5.71 (2 H, m, AA′ part of a AA′BB′C spin system, H$_{ortho}$)[f] 6.68 (2 H, BB′ part of a AA′BB′C spin system, $^3J_{HH}$ 8.1, $^3J_{HH}$ 7.6, $^4J_{HP}$ 2.3, H$_{meta}$) 7.53 (2 H, m, H$_{ortho}$)[f] 7.58−7.70 (5 H, m, H$_{ortho}$/H$_{meta}$/H$_{para}$)[g] 7.78 (2 H, BB′ part of a AA′BB′C spin system, $^3J_{HH}$ 9.5, $^3J_{HH}$ 7.7, $^4J_{HP}$ 1.9, H$_{meta}$) 7.89 (1 H, m, H$_{para}$)[f]

[a] In all cases the isomers with the specification **a** are the major diastereomers of the equilibrium mixture in solution. Units are δ, with J in Hz. Legend: s = singlet, d = doublet, q = quartet, m = multiplet, br = broad signals. In all cases SiMe$_4$ is the standard. Signal assignment is on the basis of two-dimensional ^{1}H, ^{1}H and ^{1}H, ^{13}C correlation spectroscopy. [b] LL* = (*S*)-*N*-(1-phenylethyl)pyrrolecarbaldiminate, L′ = Cl for **1a**,**b** and PPh$_3$ for **2a**,**b**. [c] At 400 MHz, in CDCl$_3$, and at −20 °C. The signals for **1b** are taken from the equilibrium spectrum measured at room temperature. [d] Pyr = aromatic ABC system (pyrrole part) of the chelating ligand. [e] At 400 MHz, in acetone-d_6, and at 21 °C. [f] $^nJ_{HP}$ was determined by hydrogen phosphorus decoupling. [f] $^4J_{HH}$, $^3J_{HH}$, or $^3J_{HP}$ not determined due to line broadening. [g] These signals overlap partially. [h] At 400 MHz, in acetone-d_6, and at −80 °C. [i] The signal for one H$_{para}$ of the PPh$_3$ ligand is hidden by this H$_{meta}$ Ph signal.

in which LL* = anion of (*S*)-*N*-(1-phenylethyl)pyrrolecarbaldimine.[11] It will be shown that the N,N donor set of the 2-(*S*)-*N*-(1-phenylethyl)pyrrolecarbaldiminato anion confers an appreciably increased configurational stability on the ruthenium atom.

Results and Discussion

Synthesis and Characterization of the Diastereomeric Chloro Complexes 1a and 1b. (*S*)-*N*-(1-Phenylethyl)pyrrolecarbaldimine (HLL*), used throughout this study, was prepared from 2-pyrrolecarbaldehyde and (*S*)-(1-phenylethyl)amine. Deprotonation of HLL* was carried out with NaH in dichloromethane at 0 °C. To the solution of the sodium salt NaLL* the dimer [(η^6-C_6H_6)RuCl$_2$]$_2$ was added. The diastereomeric chloro complexes (S_{Ru},S_C)- and (R_{Ru},S_C)-[(η^6-C_6H_6)Ru(LL*)Cl] (**1a**,**b**), differing in the configuration of the stereogenic ruthenium atom, were formed (Scheme 1).

Scheme 1

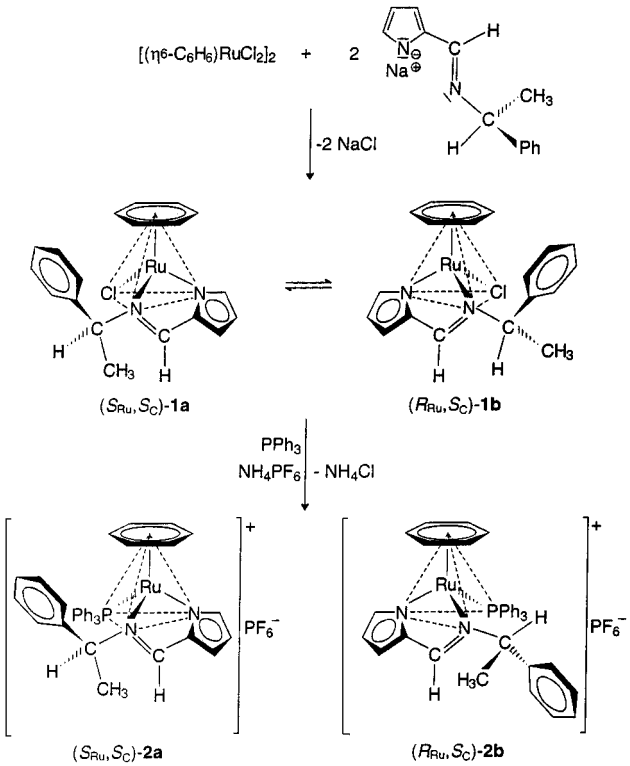

The mixture of diastereomers **1a** and **1b** was purified by column chromatography on silica gel with dichloromethane/ethyl acetate (1:1) and by precipitation from the eluate with petroleum ether. Integration of the doublet signals for the methyl protons of the 1-phenylethyl group at 1.75 and 1.98 ppm in the room-temperature ^{1}H NMR spectrum of the diastereomer mixture showed the ratio **1a**:**1b** = 68:32 at this stage of the purification procedure (Table 1). Surprisingly, the signal splitting of 0.04 ppm for the η^6-benzene protons is much smallar than for the corresponding (*S*)-*N*-(1-phenylethyl)salicylaldiminato complexes.[12,14]

The crystallization of the diastereomer mixture **1a**,**b** from chloroform/petroleum ether (2:1) at 5 °C gave orange prisms of X-ray analytical quality. Elemental analysis, ^{1}H NMR spectra (Table 1), and IR spectra showed that the crystals contain 1 equiv of CHCl$_3$ in the unit cell. The ^{1}H NMR spectrum measured at −25 °C of a CDCl$_3$ solution of these crystals which had been prepared at −30 °C exhibited only the signals of the diastereomer **1a** with the high-field signal at 1.75 ppm

Table 2. Chiroptical Data of the Complexes (S_{Ru},S_C)-1a, (S_{Ru},S_C)-2a, and (R_{Ru},S_C)-2b[a]

complex	**1a**[b]	**2a**[c]	**2b**[c]
	(i) CD Data		
c (10^4 mol L^{-1})	13.7	3.22	3.22
λ_{max} (nm)/$\Delta\epsilon$	373/−0.6	260/−30.2	260/7.9
(dm^3 mol^{-1} cm^{-1})	387/−1.9	295/6.0	295/−8.2
	425/14.7	335/−5.4	340/6.5
		376/−10.8	
λ_0 (nm)[d]	354, 365, 398	284, 315	277, 319
	(ii) Optical Rotation		
c (g/100 mL of solution)	0.08	0.08	0.08
$[\alpha]_D$	+98	−493	+154
$[\alpha]_{578}$	+132	−530	+166
$[\alpha]_{546}$	+333	−676	+214

[a] In all cases CH_2Cl_2 was used as solvent. [b] CD data measured at −20 °C, optical rotations measured at −25° due to the configurational lability. [c] CD data and optical rotations measured at 20 °C. [d] λ_0 is the wavelength where the spectra cross the zero line.

for the methyl protons. When the solution was warmed, the signals for the other diastereomer **1b** appeared slowly at a temperature above 0 °C. Therefore, during crystallization of diastereomer **1a** an asymmetric transformation of the second kind[18] must have occurred, providing diastereomerically pure **1a** in yields higher than expected on the basis of its equilibrium concentration in solution. The room-temperature ^{1}H NMR spectrum in $CDCl_3$ shows a thermodynamic equilibrium ratio of the diastereomers **1a**:**1b** = 68:32.

Epimerization 1a ⇌ 1b. The conversion of **1a** into the equilibrium mixture **1a** ⇌ **1b** was followed in $CDCl_3$ solution by ^{1}H NMR spectroscopy. To determine the ratio **1a**:**1b**, the methyl doublet signals were integrated. Analysis was performed with the function $\ln\{([A_0] - [A_\infty])/([A] - [A_\infty])\} = (\ln 2/k)t = \tau_{1/2}t$. The sample was thermostated at 27.0 ± 0.3 °C. The ^{1}H NMR spectra were recorded at about −25 °C after the sample had been immersed into a bath of −60 °C to stop the reaction. According to this protocol, 13 different measurements were carried out. The reaction turned out to be of first or pseudo-first order, and no decomposition products could be detected. The equilibrium ratio at 27.0 ± 0.3 °C, measured after 18 h of thermostating, was **1a**:**1b** = 68.1:31.9. The half-life of the approach to the equilibrium **1a** ⇌ **1b** in $CDCl_3$ at 27.0 ± 0.3 °C is $\tau_{1/2}$ = 9.2 ± 0.1 min. For the analogous chloro complex derived from the chiral salicylaldiminato ligand, the corresponding isomerization reaction was fast even at −80 °C.[12,14] Thus, the exchange of the donor atom set N,O for N,N in the pyrrolealdiminato derivatives **1a**,**b** is associated with a remarkable increase of the configurational stability at the ruthenium atom. In Table 2 the CD data are summarized. The $^{13}C\{^1H\}$ NMR data are given in Table 3.

Crystal Structure of the Diastereomer 1a. In order to determine the absolute configuration of **1a**, a single-crystal X-ray diffraction analysis was carried out. Details of the structure analysis and the crystal data are listed in Table 4. Selected bond distances and angles are given in Table 5. One equivalent of $CHCl_3$ is contained in the unit cell. In Figure 1 an ORTEP plot of the molecular structure of **1a** is shown.

In **1a**, the chiral carbon atom of the chelate ligand has the expected S_C configuration and the stereogenic

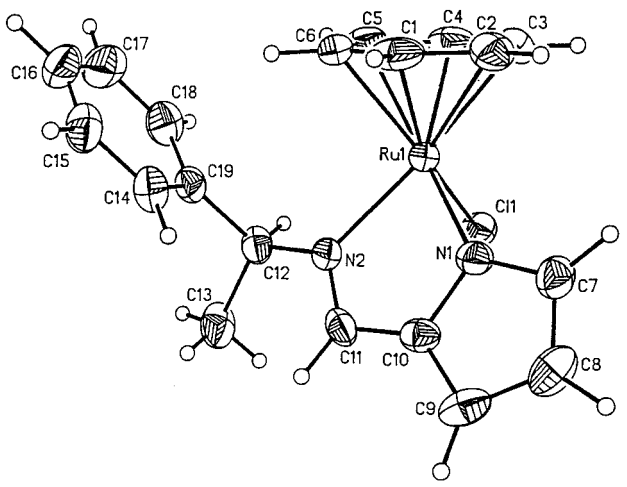

Figure 1. ORTEP representation of the crystal structure of (S_{Ru},S_C)-[(η^6-C_6H_6)Ru(LL*)Cl] (**1a**) with the thermal ellipsoids at the 40% probability level.

ruthenium center has an S_{Ru} configuration, specified with the priority sequence η^6-C_6H_6 > Cl > N(imine of LL*) > N(pyrrolate of LL*).[19−21] The pyrrolecarbaldiminato chelate ring of **1a** is only five-membered, whereas the chelate ring in the corresponding salicylaldiminato complex is six-membered.[14] As a consequence, the angle N(1)−Ru(1)−N(2) (77.1°) in **1a** is significantly smaller than the corresponding angle in the salicylaldiminato complex (86.5°). The bond length Ru(1)−N(1) from ruthenium to the pyrrolate nitrogen is about 0.06 Å shorter than the bond length Ru(1)−N(2) to the imine nitrogen. Although N-donor ligands have only small *trans* effects, the bond length Ru(1)−C(5) to the carbon atom C(5) of the η^6-benzene ligand *trans* to N(1) is about 0.06 Å shorter than the other bond lengths Ru(1)−C(1−4) and Ru(1)−C(6). In the crystal structure of **1a** there are no nonbonding distances smaller than the van der Waals radii.[22,23]

The face-on orientation of the phenyl substituent of the 1-phenylethyl group with respect to the η^6-benzene ligand is the consequence of an attractive interaction called the "β-phenyl effect", a $\pi-\pi$ edge-to-face or T-shaped interaction.[12,14,24−28] The medium distance between the carbon atoms C(14), C(18), and C(19) of the phenyl substituent and C(6) of the η^6-benzene ligand is only 3.39 Å. In previously reported (arene)ruthenium salicylaldiminato complexes the thermodynamically more stable diastereomers also showed this face-on orientation of the phenyl substituent in the crystal structures.[12,14] As this face-on arrangement was retained in solution, the ^{1}H NMR signals of the η^6-benzene

(18) Eliel, E. L.; Wilen, S. H.; Mander, L. N. *Stereochemistry of Organic Compounds*; Wiley-Interscience: New York, 1994; p 365.

(19) Cahn, R. S.; Ingold, C. K.; Prelog, V. *Angew. Chem.* **1966**, *78*, 413; *Angew. Chem., Int. Ed. Engl.* **1966**, *5*, 385.
(20) Lecomte, C.; Dusausoy, Y.; Protas, J.; Tirouflet, J. *J. Organomet. Chem.* **1974**, *73*, 67.
(21) Stanley, K.; Baird, M. C. *J. Am. Chem. Soc.* **1975**, *97*, 6599.
(22) Allinger, N. L.; Chung, D. Y. *J. Am. Chem. Soc.* **1976**, *98*, 6798.
(23) Charton, M.; Motoc, I. *Top. Curr. Chem.* **1983**, *114*, 1.
(24) Brunner, H. *Angew. Chem.* **1983**, *95*, 921; *Angew. Chem., Int. Ed. Engl.* **1983**, *22*, 897.
(25) Hunter, C. A.; Sanders, J. K. M. *J. Am. Chem. Soc.* **1990**, *112*, 5525.
(26) Hunter, C. A.; Singh, J.; Thornton, J. M. *J. Mol. Biol.* **1991**, *218*, 837.
(27) Armspach, D.; Ashton, P. R.; Moore, C. P.; Spencer, N.; Stoddart, J. F.; Wear, T. J.; Williams, D. J. *Angew. Chem.* **1993**, *105*, 944; *Angew. Chem., Int. Ed. Engl.* **1993**, *32*, 854.
(28) Jorgensen, W. L.; Severane, D. L. *J. Am. Chem. Soc.* **1990**, *112*, 4768.

Table 3. $^{13}C\{^1H\}$ NMR Data of the Complexes (S_{Ru},S_C)-[(η^6-C_6H_6)Ru(LL*)Cl] (1a), (S_{Ru},S_C)-[(η^6-C_6H_6)Ru(LL*)(PPh$_3$)]PF$_6$ (2a), and (R_{Ru},S_C)-[(η^6-C_6H_6)Ru(LL*)(PPh$_3$)]PF$_6$ (2b)[a]

complex	LL*[b]	η^6-C_6H_6	L′[b]
1a[c]	25.4 ($CHCH_3$), 70.0 ($CHCH_3$), 112.7 (C^4 Pyr), 116.2 (C^3 Pyr), 126.4 (C_{meta} Ph), 127.8 (C_{para} Ph), 129.1 (C_{ortho} Ph), 138.3 (C^5 Pyr), 139.2 (C^2 Pyr), 144.0 (C_{ipso} Ph), 155.9 (N=CH)	83.3	
2a[d]	25.4 ($CHCH_3$), 72.9 ($CHCH_3$), 114.3 (d, $^4J_{CP}$ 1.9, C^4 Pyr), 119.1 (C^3 Pyr), 127.2 (C_{ortho} Ph), 129.0 (C_{para} Ph), 130.1 (C_{meta} Ph), 142.6 (d, $^3J_{CP}$ 2.0, C^2 Pyr), 143.2 (d, $^3J_{CP}$ 2.9, C^5 Pyr), 144.6 (C_{ipso} Ph), 159.9 (N=CH)	91.6 (d, $^2J_{CP}$ 2.9)	129.6 (d, $^3J_{CP}$ 10.2, C_{meta}), 130.8 (d, $^1J_{CP}$ 48.5, C_{ipso}), 132.2 (d, $^4J_{CP}$ 2.6, C_{para}), 134.8 (d, $^2J_{CP}$ 10.1, C_{ortho})
2b[e,f]	24.8 ($CHCH_3$), 71.8 ($CHCH_3$), 113.7 (C^4 Pyr), 117.8 (C^3 Pyr), 128.1 (C_{meta} Ph), 128.4 (C_{para} Ph), 129.2 (C_{ortho} Ph), 141.5 (C^5 Pyr), 141.9 (C^2 Pyr), 142.2 (C_{ipso} Ph), 161.0 (N=CH)	91.5 (d, $^2J_{CP}$ 2.0)	126.1 (d, $^1J_{CP}$ 47.1, C_{ipso}), 127.8 (d, $^2J_{CP}$ 8.8, C_{meta}), 129.4 (d, $^2J_{CP}$ 9.6, C_{meta}), 129.8 (d, $^2J_{CP}$ 10.1, C_{meta}), 130.0 (C_{para}), 131.5 (d, $^1J_{CP}$ 48.7, C_{ipso}), 132.0 (C_{para}), 132.6 (d, $^1J_{CP}$ 48.7, C_{ipso}), 132.6 (d, C_{ortho})[g] 134.6 (d, $^2J_{CP}$ 8.8, C_{ortho}), 135.7 (d, $^2J_{CP}$ 10.7, C_{ortho})

[a] Units of δ, with J in Hz; d = doublet. In all cases $SiMe_4$ is the standard. Signal assignment is on the basis of two-dimensional $^1H,^1H$ and $^1H,^{13}C$ correlation spectroscopy. [b] LL* = (*S*)-*N*-(1-phenylethyl)pyrrolecarbaldiminate, L′ = Cl for **1a** and PPh_3 for **2a** and **2b**. [c] At 100.6 MHz, in $CDCl_3$, and at −20 °C. [d] At 100.6 MHz, in acetone-d_6, and at 21 °C. [e] At 100.6 MHz, in acetone-d_6, and at −80 °C. [f] All the PPh_3 signals coalesce at about −20 °C. [g] $^2J_{CP}$ not determined due to line broadening.

Table 4. Summary of Crystal Data, Data Collection, and Structure Refinement for the Complexes (S_{Ru},S_C)-[(η^6-C_6H_6)Ru(LL*)Cl]·$CHCl_3$ (1a), (S_{Ru},S_C,P_{PPh_3})-[(η^6-C_6H_6)Ru(LL*)(PPh$_3$)]PF$_6$ (2a), and (R_{Ru},S_C,P_{PPh_3})-[(η^6-C_6H_6)Ru(LL*)(PPh$_3$)]PF$_6$ (2b)[a]

	1a	2a	2b
	(i) Crystal Parameters		
elemental formula	$C_{19}H_{19}ClN_2Ru{\cdot}CHCl_3$	$C_{37}H_{34}F_6N_2P_2Ru$	$C_{37}H_{34}F_6N_2P_2Ru$
fw	531.27	783.70	783.70
cryst color, shape	orange prisms	yellow prisms	yellow needles
cryst size (mm)	0.40 × 0.40 × 0.95	0.22 × 0.37 × 0.67	0.10 × 0.15 × 0.90
cryst syst	rhombic	monoclinic	tetragonal
space group (No.)	$P2_12_12_1$ (No. 19)	$P2_1$ (No. 4)	$P1$ (No. 1)
a (Å)	9.856(7)	13.600(8)	9.799(2)
b (Å)	12.40(1)	17.84(1)	10.379(4)
c (Å)	17.34(3)	14.71(1)	10.831(4)
α (deg)	90	90	90
β (deg)	0	97.40(6)	90
γ (deg)	90	90	90
V (Å^3)	2118.4	3539.3	3464.5
Z	4	2 × 2	4
D_{calcd} (g cm^{-3})	1.66	1.47	1.50
F(000)	1064	1592	1592
μ (mm^{-1})	1.24	0.58	0.59
	(ii) Data Collection		
hkl ranges	0−13, 0−16, 0−22	−16 to +16, 0−22, 0−18	0−11, 0−11, 0−11
2θ range (deg)	3.0−52.5	3.0−55.5	3.0−42.5
total no. of unique reflns	4226	7412	2284
no. of obsd rflns ($I > 2.5\sigma_I$)	3249	3914[b]	1418
min, max transmissn factors	0.86, 1.00	0.83, 1.00	0.85, 1.00
	(iii) Data Refinement		
no. of rflns and 2θ range (deg) for the empirical abs cor	7, 8.0−46.0	6, 7.4−37.0	5, 4.6−28.0
no. of LS params	245	202 + 203 + 128[c]	234
largest shift/esd in final cycle	0.003	0.02	0.03
$\Delta\rho_{min}$, $\Delta\rho_{max}$ (e Å^{-3})	−0.52, 0.68	−0.40, 0.46	−0.72, 0.87
R (=$\sum\|\|F_o\| - \|F_c\|\|/\sum\|F_c\|$)	0.039	0.052	0.078
R_w (=$\sum\|\|F_o\| - \|F_c\|\|w^{1/2}/\sum\|F_o\|w^{1/2}$, $w = 1/\sigma^2(F_o)$)	0.034	0.040	0.064

[a] Details in common: Syntex-Nicolet R3 diffractometer; Mo Kα radiation (λ = 0.710 73 Å); 293 K; graphite crystal monochromator; structure solution by Patterson−Fourier methods with SHELXTL PLUS, release 4.11/V programs,[42] on a MicroVAX II computer. Positional parameters of the H atoms were calculated by the option HFIX and were not refined. [b] Numbers of reflections with $I > 2.0\sigma(I)$: 4294. [c] Refinement of data in three blocks.

ligands were high-field shifted due to the magnetic anisotropy of the phenyl substituent. For the less stable diastereomers the steric hindrance of the methyl group of the 1-phenylethyl substituent with the monodentate ligand prevented this face-on orientation. Consequently, there was no high-field shift of the ^1H NMR signals of the corresponding η^6-benzene ligand.[12,14] In contrast, the η^6-benzene signals of the two diastereomers **1a**,**b** show only a chemical shift difference of 0.04 ppm (Table 1). The smaller chelate ring of the pyrrolecarbaldiminato ligand may be the reason for the smaller steric hindrance of the methyl group of the 1-phenylethyl substituent with the chloro ligand.

Synthesis of the Diastereomeric Triphenylphosphane Complexes 2a and 2b. Finely ground **1a** and triphenylphosphane were stirred in methanol at −15 °C. Dissolution required about 90 min. Concomitantly, the chloro ligand in **1a** was substituted for triphenylphosphane (Scheme 1). Then, a solution of NH_4PF_6 in ice-cold water was added to exchange the chloride anion for the PF_6 anion. Precipitation of the diastereomeric phosphane complexes (S_{Ru},S_C)- and (R_{Ru},S_C)-[(η^6-C_6H_6)Ru(LL*)(PPh$_3$)]PF$_6$ (**2a**,**b**) was completed by water. The product mixture was purified by dissolution in acetone and precipitation with petroleum ether. The yellow precipitate was isolated in 86−94% yield. The

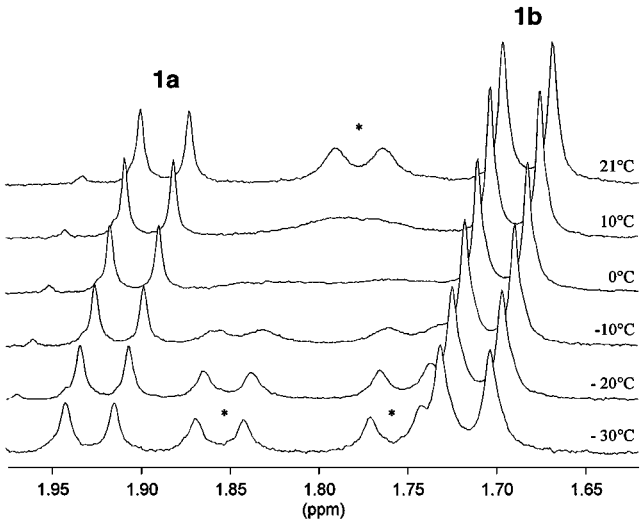

Figure 2. ^{1}H NMR spectra between 2.00 and 1.55 ppm (methyl doublet region) of **1a** in methanol-d_4 at various temperatures. The horizontal offset of the spectra is 0.015 ppm.

Table 5. Selected Bond Lengths (Å) and Angles (deg) for the Complex (S_{Ru},S_C)-[(η^6-C_6H_6)Ru(LL*)Cl]·$CHCl_3$ (1a)

Bond Lengths (Å)			
Ru(1)−Cl(1)	2.396(4)	Ru(1)−N(1)	2.037(6)
Ru(1)−C(1)	2.153(8)	Ru(1)−N(2)	2.101(5)
Ru(1)−C(2)	2.156(7)	C(11)−N(2)	1.278(7)
Ru(1)−C(3)	2.166(7)	C(10)−N(1)	1.367(8)
Ru(1)−C(4)	2.151(8)	N(2)−C(12)	1.466(7)
Ru(1)−C(5)	2.208(7)	N(2)−C(12)	1.466(7)
Ru(1)−C(6)	2.151(8)		

Bond Angles (deg)			
N(1)−Ru(1)−N(2)	77.1(2)	C(1)−Ru(1)−C(2)	37.9(3)
Cl(1)−Ru(1)−N(2)	82.6(2)	C(2)−Ru(1)−C(3)	37.0(3)
Cl(1)−Ru(1)−N(1)	87.6(2)	C(3)−Ru(1)−C(4)	37.8(3)
Ru(1)−N(1)−C(10)	115.3(4)	C(4)−Ru(1)−C(5)	37.0(3)
N(1)−C(10)−C(11)	114.6(5)	C(5)−Ru(1)−C(6)	37.0(3)
C(10)−C(11)−N(2)	118.1(6)	C(1)−Ru(1)−C(6)	37.7(3)
Ru(1)−N(2)−C(11)	114.7(4)		

ratio of **2a**:**2b** was 1:1, as determined by integration of the methyl signals in the ^{1}H NMR spectrum in acetone-d_6 at about −70 °C. However, it does not change by warming up the acetone-d_6 solutions to 50 °C for hours. Therefore, similar to the (arene)ruthenium salicylaldiminato complexes,[12−14] the substitution of the chloride ligand in **1a** proceeded without retaining the ruthenium configuration.

To further elucidate the course of the substitution reaction, the behavior of **1a** was examined in the solvent methanol-d_4. The sample was measured in the temperature range of −30 to +21 °C by ^{1}H NMR spectroscopy (Figure 2). In addition to the doublets of the methyl group of the two diastereomers **1a**,**b,** at −30 °C the doublets of the methyl groups of another two species, marked with asterisks, were observed in a ratio of about 1:1 (Figure 2). When the sample was warmed, the marked doublets coalesced at about 0 °C and at 21 °C only one broad doublet signal resulted, while the shape of the signals of the diastereomers **1a**,**b** did not change. This behavior of **1a,b** in methanol solution can be explained by the formation of configurationally labile solvate complexes after dissociation of the chloro ligand. The barrier to inversion of the ruthenium configuration of $\Delta G^{\ddagger}_{273}$ = 57.6 ± 0.8 kJ mol^{-1} in these solvate complexes can be obtained from the coalescence spectrum.[29]

Separation and Single-Crystal Breeding of the Diastereomers 2a and 2b. From a solution of the mixture of (S_{Ru},S_C)- and (R_{Ru},S_C)-[(η^6-C_6H_6)Ru(LL*)-(PPh_3)]PF_6 (**2a**,**b** ratio 1:1) in dichloromethane/*n*-hexane (1:2) yellow needles of **2b** of X-ray quality crystallized in yields up to 60% with respect to its content in the mixture used for crystallization. The ^{1}H NMR spectrum of a solution of the crystals in acetone-d_6 in the temperature range of −80 to +50 °C showed only the low-field signal of **2b** for the η^6-benzene ligand, indicating diastereomeric purity of the yellow needles (see below and Table 1).

From the mother liquor the remaining diastereomer mixture was precipitated quantitatively by addition of petroleum ether. The dry precipitate was dissolved in acetone/methanol, and water was added to the solution. After the mixture stood for 3 days at 5 °C, the resulting precipitate was dried and dissolved in dichloromethane. Addition of *n*-hexane up to a dichloromethane/*n*-hexane ratio of 5:4 effected the formation of yellow prisms of **2a** in 51% yield. An acetone-d_6 solution of the crystals showed only the high-field signal of **2a** for the η^6-benzene ligand, indicating diastereomeric purity of the yellow prisms (see below and Table 1).

NMR Spectroscopic Properties of the Diastereomers 2a and 2b. The prismatic crystals of diastereomer **2a** exhibited the high-field ^{1}H NMR signal for the η^6-benzene ligand in acetone-d_6 at 5.68 ppm (Table 1). The doublet for the methyl group of the N substituent appeared at 1.05 ppm and the quartet for the methine proton at 5.30 ppm. In the range of 6.17−7.35 ppm the signals for the pyrrole protons were observed. The signals of the triphenylphosphane protons were split in three multiplets at 7.21, 7.50−7.53, and 7.60 ppm. The signals for the *ortho* and *para* protons were analyzed according to first-order-coupling spin systems (Table 1). When the acetone-d_6 solution of **2a** was cooled to −80 °C, the signals of the triphenylphosphane protons broadened significantly but did not coalesce.[11] A broadening was also observed for the corresponding ^{13}C{^{1}H} NMR signals of the triphenylphosphane carbon atoms (Table 3). It must be concluded that the steric restrictions in the molecular structure of the cation of **2a** are not large enough to stop the rotation of the triphenylphosphane ligand about the ruthenium−phosphorus bond on cooling.

The yellow needles of diastereomer **2b** exhibited the low-field ^{1}H NMR signal for the η^6-benzene ligand in acetone-d_6 at 6.37 ppm (Table 1). The doublet for the methyl group of the N substituent appeared at 1.87 ppm and the quartet for the methine proton at 5.46 ppm. The signals for the pyrrole protons were observed at 6.11, 6.36, and 7.58−7.70 ppm. In contrast to the spectrum of **2a**, the triphenylphosphane ligand of diastereomer **2b** showed at room temperature three very broad multiplets for the *ortho, meta,* and *para* protons. These signals sharpened a little on warming the sample to 50

(29) Friebolin, H. *Ein- und zweidimensionale NMR-Spektroskopie*; VCH: Weinheim, Germany, 1992; p 293.

°C, and they coalesced in the temperature range of 0 to −20 °C. Further cooling of the acetone-d_6 solution of **2b** effected a splitting into well-resolved signals for the *ortho*, *meta*, and *para* protons. The splitting pattern indicated a freezing of the rotation of the triphenylphosphane ligand about the ruthenium−phosphorus bond.[30−35] The ^{1}H NMR signals of one of the triphenylphosphane phenyls showed a strong high-field shift. At 5.71 ppm a multiplet for two *ortho* protons, at 6.68 ppm a multiplet for two *meta* protons, and at 7.21 ppm a multiplet for the *para* proton superposed by the signal of the *meta* protons of the phenyl substituent of the chelate ring were observed.[11] The ^{13}C{^{1}H} NMR spectrum changed in a similar manner on cooling **2b** in acetone-d_6 to −80 °C (Table 3).[11] Thus, the steric restrictions in the molecular structure of the cation of **2b** are large enough to stop the rotation of the triphenylphosphane ligand about the ruthenium−phosphorus bond on cooling.

On the other hand, there was no coalescence of the signals of the phenyl substituent of the 1-phenylethyl group for both diastereomers **2a** and **2b** in the measured temperature range, and the line width of the ^{31}P{^{1}H} NMR signals was not affected by cooling. In contrast to the diastereomers **1a**,**b,** the high-field shift of the signal for the η^6-benzene ligand of diastereomer **2a** at 5.68 ppm in comparison to diastereomer **2b** at 6.37 ppm indicates a significant "β-phenyl effect".[24−28]

Epimerization 2a ⇌ 2b. Surprisingly, even in boiling acetone-d_6 the optically pure compounds **2a** and **2b** did not interconvert. However, in nitromethane-d_3 at 85.0 ± 0.3 °C epimerization took place. With **2b** as starting material, 19 measurements were carried out according to the following protocol.[11] The sample was thermostated at 85 °C for a given period of time. Then, the reaction was stopped by immersing the sample into an ice bath. The subsequent ^{1}H NMR spectrum was measured at 21 °C. The signals of the methyl protons of the 1-phenylethyl group were integrated. After 18 h of heating to 85 °C, the equilibrium ratio in nitromethane-d_3 was determined to be **2a**:**2b** = 93.5:6.5. The epimerization turned out to be a clean first-order reaction. The half-life of the approach to the equilibrium **2a** ⇌ **2b** in nitromethane-d_3 was $\tau_{1/2}$ (min) = 58.2 ± 0.4. Thus, different from the salicylaldiminato ligand system,[12,14] the pyrrolealdiminato ligand system confers a remarkable configurational stability on the ruthenium atom in [(η^6-C_6H_6)Ru(LL*)(PPh_3)]PF_6 (**2a,b**).

Crystal Structures of the Diastereomers 2a and 2b. The crystal structures of diastereomerically pure **2a** and **2b** were determined using a yellow prism of **2a** and a yellow needle of **2b**. In Table 4 details of the structure determination and the crystal data are listed. Selected bond distances and angles are given in Tables 6 and 7. In Figure 3 ORTEP plots of the molecular structures of the cations **A** and **B** of complex **2a** are shown; in Figure 4 an ORTEP plot of the crystal structure of the cation of diastereomer **2b** is shown.

In the unit cell of diastereomer **2a**, the two independent cations **A** and **B** with the same (S_C) configuration of the chiral *N*-(1-phenylethyl)pyrrolecarbaldiminato ligand were located. The ruthenium configuration in both cations is S_{Ru}, as specified with the priority sequence η^6-C_6H_6 > PPh_3 > N(imine of LL*) > N(pyrrolate of LL*).[19−21] The structures of the two cations differ in the arrangement of the η^6-benzene ligand, which in **B** is rotated by about 30° compared with **A**. The dihedral angles defining the conformation of the triphenylphosphane ligand deviate in **A** and **B** by a maximum of only about 4°. Accordingly, the triphenylphosphane ligands in both cations of **2a** have the same + sense of helicity.[12,14,36−38] Thus, diastereomer

Table 6. Selected Bond Lengths (Å) and Angles (deg) for the Complex (S_{Ru},S_C,P_{PPh_3})-[(η^6-C_6H_6)Ru(LL*)(PPh_3)]PF_6 (2a)

Bond Lengths (Å)			
Ru(1)−P(1)	2.362(3)	Ru(2)−P(2)	2.362(4)
Ru(1)−N(1)	2.059(9)	Ru(2)−N(3)	2.090(11)
Ru(1)−N(2)	2.114(9)	Ru(2)−N(4)	2.062(9)
Ru(1)−C(1)	2.217(16)	Ru(2)−C(41)	2.212(15)
Ru(1)−C(2)	2.192(17)	Ru(2)−C(42)	2.249(15)
Ru(1)−C(3)	2.213(21)	Ru(2)−C(43)	2.164(13)
Ru(1)−C(4)	2.210(22)	Ru(2)−C(44)	2.190(17)
Ru(1)−C(5)	2.202(16)	Ru(2)−C(45)	2.239(16)
Ru(1)−C(6)	2.224(14)	Ru(2)−C(46)	2.223(18)
N(1)−C(34)	1.345(16)	N(3)−C(75)	1.273(15)
C(34)−C(35)	1.433(16)	C(74)−C(75)	1.377(18)
N(2)−C(35)	1.306(13)	N(4)−C(74)	1.345(17)
N(2)−C(36)	1.490(14)	N(3)−C(76)	1.496(16)
Bond Angles (deg)			
N(1)−Ru(1)−N(2)	77.5(3)	N(3)−Ru(2)−N(4)	76.8(4)
N(1)−Ru(1)−P(1)	88.7(3)	P(2)−Ru(2)−N(3)	88.6(3)
N(2)−Ru(1)−P(1)	87.9(2)	P(2)−Ru(2)−N(4)	87.3(3)
Ru(1)−N(1)−C(34)	115.3(7)	Ru(2)−N(4)−C(74)	115.1(8)
N(1)−C(34)−C(35)	115.7(10)	N(4)−C(74)−C(75)	113.8(11)
N(2)−C(35)−C(34)	117.1(10)	N(3)−C(75)−C(74)	121.0(12)
Ru(1)−N(2)−C(35)	114.2(7)	Ru(2)−N(3)−C(75)	113.2(9)
C(1)−Ru(1)−C(2)	35.3(7)	C(41)−Ru(2)−C(42)	35.9(7)
C(2)−Ru(1)−C(3)	35.7(10)	C(42)−Ru(2)−C(34)	36.9(6)
C(3)−Ru(1)−C(4)	36.3(9)	C(43)−Ru(2)−C(44)	37.7(6)
C(4)−Ru(1)−C(5)	35.2(7)	C(44)−Ru(2)−C(45)	37.0(7)
C(5)−Ru(1)−C(6)	36.9(7)	C(45)−Ru(2)−C(46)	35.3(7)
C(1)−Ru(1)−C(6)	35.8(7)	C(41)−Ru(2)−C(46)	37.0(7)

Table 7. Selected Bond Lengths (Å) and Angles (deg) for the Complex (R_{Ru},S_C,P_{PPh_3})-[(η^6-C_6H_6)Ru(LL*)(PPh_3)]PF_6 (2b)

Bond Lengths (Å)			
Ru(1)−P(1)	2.360(7)	Ru(1)−C(29)	2.231(30)
Ru(1)−N(1)	2.058(19)	Ru(1)−C(30)	2.170(30)
Ru(1)−N(2)	2.100(21)	N(2)−C(35)	1.292(36)
Ru(1)−C(25)	2.200(27)	C(34)−C(35)	1.364(37)
Ru(1)−C(26)	2.243(34)	N(1)−C(34)	1.371(32)
Ru(1)−C(27)	2.209(29)	N(2)−C(36)	1.458(31)
Ru(1)−C(28)	2.154(30)		
Bond Angles (deg)			
N(1)−Ru(1)−P(1)	86.8(6)	C(25)−Ru(1)−C(26)	35.8(11)
N(2)−Ru(1)−P(1)	88.3(6)	C(26)−Ru(1)−C(27)	34.7(12)
N(1)−Ru(1)−N(2)	77.4(8)	C(27)−Ru(1)−C(28)	34.1(11)
Ru(1)−N(1)−C(34)	113.8(16)	C(28)−Ru(1)−C(29)	37.5(11)
N(1)−C(34)−C(35)	115.7(24)	C(29)−Ru(1)−C(30)	37.8(12)
N(2)−C(35)−C(34)	119.7(25)	C(25)−Ru(1)−C(30)	38.8(10)
Ru(1)−N(2)−C(35)	113.3(17)		

(30) Jones, W. D.; Feher, F. J. *Inorg. Chem.* **1984**, *23*, 2376.
(31) Howell, J. A. S.; Palin, M. G.; McArdle, P.; Cunningham, D.; Goldschmidt, Z.; Gottlieb, H. E.; Hezroni-Langerman, D. *Inorg. Chem.* **1993**, *32*, 3493.
(32) Howell, J. A. S.; Palin, M. G.; McArdle, P.; Cunningham, D.; Goldschmidt, Z.; Gottlieb, H. E.; Hezroni-Langerman, D. *Organometallics* **1993**, *12*, 1694.
(33) Chudek, J. A.; Hunter, G.; MacKay, R. L.; Kremminger, P.; Schlögl, K.; Weissensteiner, W. *J. Chem. Soc., Dalton Trans.* **1990**, 2001.
(34) Davies, S. G.; Derome, A. E.; McNally, J. P. *J. Am. Chem. Soc.* **1991**, *113*, 2854.
(35) Faller, J. W.; Chase, K. J. *Organometallics* **1995**, *14*, 1592.
(36) Brunner, H.; Hammer, B.; Krüger, C.; Angermund, K.; Bernal, I. *Organometallics* **1985**, *4*, 1063.
(37) Dunne, B. J.; Morris, R. B.; Orpen, A. G. *J. Chem. Soc., Dalton Trans.* **1991**, 653.

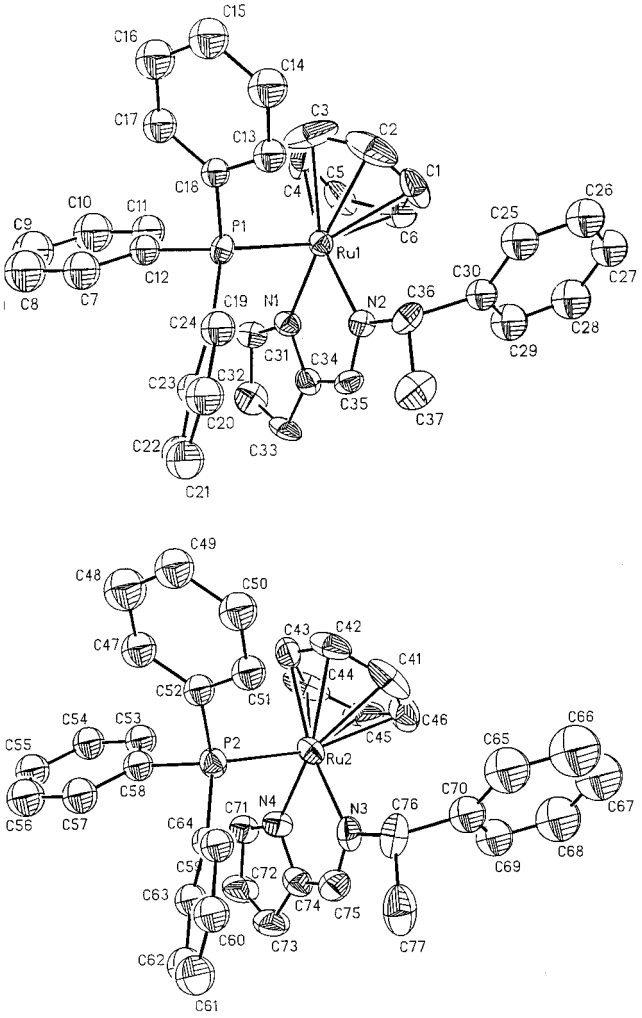

Figure 3. ORTEP representations of the crystal structures of the two independent cations **A** (upper part) and **B** (lower part) of the diastereomer (S_{Ru},S_C,P_{PPh_3})-[(η^6-C_6H_6)Ru(LL*)-(PPh_3)]PF_6 (**2a**). The hydrogen atoms and the PF_6 anions were omitted for clarity. The thermal ellipsoids are at the 40% probability level.

2a has to be formulated as (S_{Ru},S_C,P_{PPh_3})-[(η^6-C_6H_6)Ru-(LL*)(PPh_3)]PF_6.

As in the crystal structure of **1a**, in both cations of diastereomer **2a** the methine hydrogen atom (the smallest substituent of the 1-phenylethyl group) is oriented toward the sterically demanding triphenylphosphane ligand. Several nonbonding distances are significantly smaller than the sum of the van der Waals radii:[22,23] e.g., the distance between the methine hydrogen at C(36) and the hydrogen at C(19) (2.29 Å) and the distance between the hydrogen at C(11) and the hydrogen at C(4) of the η^6-benzene ligand (2.22 Å). In both cations of **2a** the phenyl substituents of the 1-phenylethyl groups (C(25)−C(30) in cation **A** and C(65)−C(70) in cation **B**) adopt a face-on orientation with respect to the η^6-benzene ligand. Assuming that the structure found in the solid state also represents an energy minimum in solution as far as the conformation of the 1-phenylethyl group is concerned, the high-field shift of the ^{1}H NMR signal at 5.68 ppm of the η^6-benzene ligand in **2a** can be explained by an attractive "β-phenyl effect".[12,14,24−28]

(38) Garner, S. E.; Orpen, A. G. *J. Chem. Soc., Dalton Trans.* **1993**, 533.

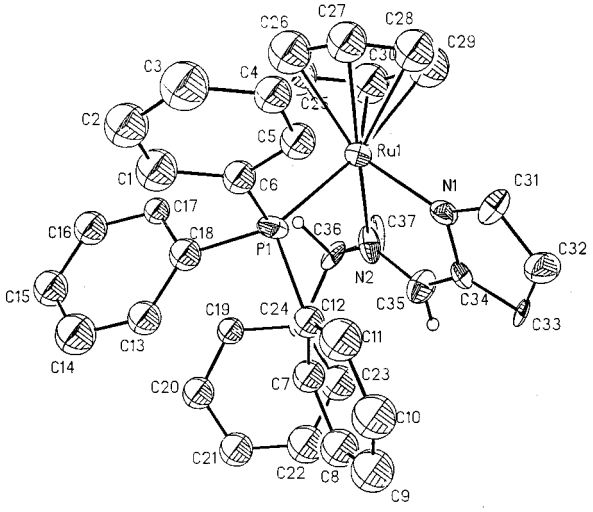

Figure 4. ORTEP representation of the crystal structure of the cation of the diastereomer (R_{Ru},S_C,P_{PPh_3})-[(η^6-C_6H_6)-Ru(LL*)(PPh_3)]PF_6 (**2b**). The hydrogen atoms and the PF_6 anion were omitted for clarity, except the methine hydrogen at C(36) and the hydrogen at C(35). The thermal ellipsoids are at the 40% probability level.

The cation of diastereomer **2b** (Figure 4) is characterized by S_C and R_{Ru} configurations. A remarkable point is the identical triphenylphosphane helicities in the two cations of **2a** and in the cation of **2b**. Therefore, **2b** has to be formulated as (R_{Ru},S_C,P_{PPh_3})-[(η^6-C_6H_6)Ru(LL*)-(PPh_3)]PF_6.

In the crystal structure of **2b**, the hydrogen atom of the 1-phenylethyl group (the smallest substituent at C(36)) is oriented toward the sterically demanding triphenylphosphane ligand. The dihedral angles H(36)−C(36)−N(2)−C(35) and C(37)−C(36)−N(2)−C(35) which characterize the deviation of the substituents from the chelate plane Ru(1)−N(1)−C(34)−C(35)−N(2) are 7.1 and 111.3°. As a consequence, a face-on orientation of the phenyl substituent C(19)−C(24) with respect to the η^6-benzene ligand C(25)−C(30) in diastereomer **2b** is not possible. Thus, the η^6-benzene protons in the ^{1}H NMR spectrum of diastereomer **2b** do not show a high-field shift, such as those of diastereomer **2a**, but appear in the normal range (6.37 ppm).

From the crystal structure of diastereomer **2b**, the severe steric interaction of the triphenylphosphane phenyl rings and the 1-phenylethyl group is obvious, in accord with the restricted rotation of the triphenylphosphane ligand about the bond Ru(1)−P(1) found in the NMR spectra. This is also indicated by the small through-space distance of 2.17 Å between the hydrogen atoms at the carbon atoms C(35) and C(23).

Chiroptical Properties of 1a, 2a, and 2b. The data of the CD spectra and the optical rotations for **1a**, **2a**, and **2b** are summarized in Table 2. Due to the fast epimerization, the CD spectrum of the pure diastereomer **1a** was measured at −20 °C, whereas the chiroptical properties of the configurationally stable diastereomers **2a** and **2b** could be measured at 20 °C (Figure 5).

The CD spectra of the diastereomers **2a** and **2b** are very different from the spectrum of complex **1a** (Figure 5). Therefore, it is dangerous to establish relationships between the ruthenium configurations of different compounds only on the basis of CD spectra. Configurational

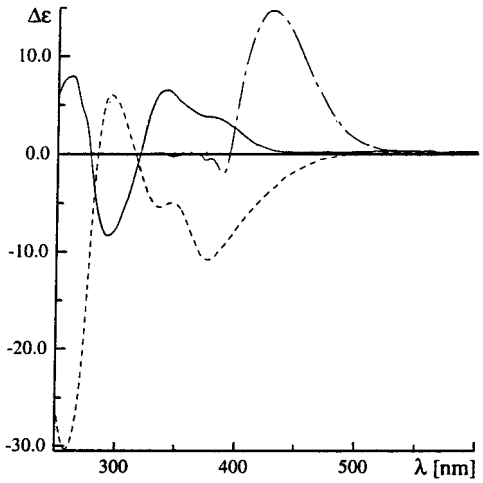

Figure 5. CD spectra of complexes **1a**, **2a** and **2b**: (− - −) **1a**, $c = 1.37 \times 10^{-3}$ mol L^{-1}, −20 °C, CH_2Cl_2; (- - -) **2a**, 3.22×10^{-4} mol L^{-1}, 20 °C, CH_2Cl_2; (—) **2b**, 3.22×10^{-4} mol L^{-1}, 20 °C, CH_2Cl_2. $\Delta\epsilon$ is in units of $dm^3\ mol^{-1}\ cm^{-1}$.

misassignments for optically active (η^6-cymene)ruthenium compounds have been published by ignoring these facts.[13,15−17]

Experimental Section

General Procedures, Solvents, and Reagents. Solvents for preparative work were dried with the appropriate reagents (methanol, activated magnesium; acetone, Sikkon (Fluka); CH_2Cl_2, Siccapent (Merck); benzene, sodium/potassium; diethyl ether, sodium/potassium; ethyl acetate, Siccapent; petroleum ether, *n*-hexane, sodium/potassium) and were saturated with dry and purified nitrogen before use by refluxing for a minimum of 3 days in a circulation apparatus. Water was saturated with nitrogen by bubbling a stream of nitrogen through it overnight. $CDCl_3$ was dried over molecular sieves (Merck, 3 Å) and saturated with dry argon before use. Acetone-d_6 and nitromethane-d_3 were saturated with argon. The samples for variable-temperature NMR measurements were prepared under nitrogen by dissolution in cold solvents using thin Schlenk tubes. The cold solutions were filled in cooled and nitrogen-flushed NMR tubes which were sealed with rubber septa. Kinetic NMR studies were performed with degassed solutions, and the NMR tubes were sealed after freezing the solutions under high vacuum. 1,3-Cyclohexadiene was purchased from Janssen Chimica (now Acros Chimica). $RuCl_3 \cdot xH_2O$ was received from Hereaus and from Degussa. Triphenylphosphane was purchased from Fluka. NH_4PF_6 was obtained from Merck. $[(\eta^6\text{-}C_6H_6)RuCl_2]_2$[39,40] and (+)-(*S*)-*N*-(1-phenylethyl)pyrrolecarbaldimine[41] were prepared by the literature method. (*S*)-(1-Phenylethyl)amine was a gift of BASF.

Spectroscopic and Analytical Methods. Elemental analyses were performed by the microanalytical laboratory of the University of Regensburg. Melting points were determined with a Büchi SMP 20 apparatus. ^1H, $^1H\{^{31}P\}$, $^{13}C\{^1H\}$, and $^{31}P\{^1H\}$ NMR spectra were measured with tetramethylsilane as internal standard and 85% H_3PO_4 as external standard, respectively, on a Bruker ARX 400 spectrometer. Circular dichroism (CD) spectra were recorded on a Jasco J-40 A spectrophotometer, and polarimetric measurements were done using a Perkin-Elmer 241 instrument. Mass spectra were measured with a Finnigan MAT 95 instrument using the field desorption method (FD).

Preparation and Crystal Breeding of the Complex (S_{Ru},S_C)-[(η^6-C_6H_6)Ru(LL*)Cl] (1a). NaH (275 mg, 11.4 mmol) was suspended in 150 mL of CH_2Cl_2 at 0 °C. After addition of a solution of (+)-(*S*)-*N*-(1-phenylethyl)pyrrolecarbaldimine (HLL*; 2.26 g, 11.4 mmol) in 50 mL of CH_2Cl_2 at 0 °C, the resulting mixture was stirred for 1 h. When the hydrogen evolution had ceased, the mixture was cooled to −15 °C, and $[(\eta^6\text{-}C_6H_6)RuCl_2]_2$ (1.90 g, 3.8 mmol) was added. After 15 h of stirring at −15 °C, the dark yellow suspension was filtered through Celite. The solvent was evaporated, and the residue was chromatographed in two portions on a cooled silica gel 60 (63−200 mesh, Merck) column (3.5 × 55 cm, −15 °C). With a 1:1 mixture of CH_2Cl_2 and ethyl acetate, a long orange band was eluted as the product zone. A thin, dark brown zone on the top was discarded together with the top of the product zone. Concentration of the product-containing solution to about 10 mL precipitated an orange, microcrystalline powder. Addition of 50 mL of diethyl ether and 200 mL of petroleum ether and standing at −30 °C for 2 days completed the precipitation. Decantation and drying gave an orange, slightly air-sensitive powder. Yield: 2.73 g (6.63 mmol, 87%). Mp: 178−181 °C dec. Anal. Calcd for $C_{19}H_{19}ClN_2Ru$: C, 55.42; H, 4.65; N, 6.80. Found: C, 55.17; H, 4.74; N, 6.81. MS (FD, CH_2Cl_2, Ru^{102}; *m*/*z* (relative intensity)): 411.9 (M^+, 100). ^1H NMR spectroscopy (Table 1) showed the two diastereomers (S_{Ru},S_C)-**1a** and (R_{Ru},S_C)-**1b** in the ratio **1a**:**1b** = 68:32, measured by integrating the two methyl signals. Crystallization of the diastereomer mixture from $CHCl_3$/petroleum ether (2:1, 23 mL of $CHCl_3$/g of **1a**,**b**) gave orange, prismatic crystals suitable for X-ray analysis. The unit cell contained 1 equiv of $CHCl_3$. ^1H NMR spectroscopy of a sample dissolved and measured at −20 °C showed only the signals of diastereomer **1a**. Yield: 2.75−3.21 g (5.18−6.03 mmol, 78−91%, refers to the product prior to crystallization). Mp: >180 °C (at about 110 °C the crystals became cloudy; they darkened at about 165 °C). Anal. Calcd for $C_{19}H_{19}ClN_2Ru \cdot CHCl_3$: C, 45.22; H, 3.79; N, 5.27. Found: C, 44.93; H, 3.87; N, 4.96. IR (KBr; cm^{-1}): 3070 (m), 3050 (w), 3025 (w) ν(C−H, arom); 2990 (m), 2960 (m), 2920, 2860 (w) ν(C−H, aliphat); 1580 (vs) ν(C=N); 1490 (w), 1455−1430 (s) ν(C=C, arom); 1390, 1330, 1290, 1270 (s); 1215−1205 (s) δ(C−H, $CHCl_3$); 1040 (vs); 830 (s); 770−730 (vs) ν_{asym}(C−Cl, $CHCl_3$); 700 (vs), 680 (s) δ(C−H, arom); 660 (m) ν_{sym}(C−Cl, $CHCl_3$); 560 (s); 370 (m), 270 (m) ν(Ru−Cl).

Preparation of the Diastereomer Mixture (S_{Ru},S_C)- and (R_{Ru},S_C)-[(η^6-C_6H_6)Ru(LL*)(PPh$_3$)]PF$_6$ (2a,b). Finely ground crystals of (S_{Ru},S_C)-[(η^6-C_6H_6)Ru(LL*)Cl] (**1a**; 1.02 g, 1.92 mmol) and of triphenylphosphane (0.56 g, 2.11 mmol) were dissolved in 200 mL of methanol at −15 to −13 °C by stirring the mixture for about 1.5 h. An ice-cold solution of NH_4PF_6 (0.63 g, 3.84 mmol) in 50 mL of water was added slowly in such a manner that the temperature of the mixture did not exceed −13 °C. The color of the solution changed from orange to yellow, and after a short time a yellow precipitate formed. The precipitation was completed by addition of 600 mL of cold water in 50 mL portions, keeping the temperature below 0 °C. The precipitate was separated by filtration and washed with 50 mL of water, 50 mL of diethyl ether, 50 mL of benzene, and 50 mL of petroleum ether. After it was dried, the yellow powder was dissolved in 20 mL of acetone and the diastereomer mixture was precipitated by addition of 100 mL of petroleum ether. After decantation, the yellow, microcrystalline powder was dried. ^1H NMR spectroscopy (Table 1) showed the two diastereomers (S_{Ru},S_C)-**2a** and (R_{Ru},S_C)-**2b** in the ratio **2a**:**2b** = 1:1 (integration of the singlets of the η^6-benzene ligand or the doublets of the methyl groups). Yield: 1.30−1.42 g (1.66−1.81 mmol, 86−94%). MS (FD, acetone, Ru^{102}; *m*/*z* (relative intensity)): 639.3 (cation of **2a**,**b**, 100). IR (KBr; cm^{-1}): 3100, 3060, 3030 (w) ν(C−H, arom); 3000, 2980, 2930 (w) ν(C−H, aliphat); 1580 (vs) ν(C=N); 1500 (w), 1440, 1400 (s) ν(C=C, arom); 1485 (m) ν(C=N); 850 (vs) ν-(P−F); 760, 745, 740, 700 (s) δ(C−H); 555 (vs) δ(P−F); 530 (vs), 510 (s), 495 (m).

(39) Winkhaus, G.; Singer, H.; Kricke, M. *Z. Naturforsch*. **1966**, *21B*, 1109.
(40) Bennett, M. A.; Huang, T.-N.; Matheson, T. W.; Smith, A. K. *Inorg. Synth*. **1982**, *21*, 75.
(41) Brunner, H.; Herrmann, W. A. *J. Organomet. Chem*. **1974**, *74*, 423.

Separation and Single-Crystal Breeding of the Diastereomer (R_{Ru},S_C,P_{PPh_3})-[(η^6-C_6H_6)Ru(LL*)(PPh_3)]PF_6 (2b). A sample (630 mg, 0.80 mmol) of the diastereomer mixture **2a**,**b** (ratio **2a**:**2b** = 1:1) was dissolved in 21 mL of CH_2Cl_2, and 10.5 mL of *n*-hexane were added. After 30 min crystallization set in and after 2 days of standing at room temperature yellow needles suitable for X-ray analysis formed. The needles were washed with a mixture of CH_2Cl_2 and petroleum ether (1:3) and petroleum ether and dried. ^{1}H NMR spectroscopy at room temperature showed only the signals of the diastereomer **2b** with the low-field singlet of the η^6-benzene protons (Table 1). Yield: 180 mg (0.23 mmol, 57% with respect to the **2b** content before crystallization). Mp: 237−240 °C dec. Anal. Calcd for $C_{37}H_{34}F_6N_2P_6Ru$: C, 56.71; H, 4.37; N, 3.58. Found: C, 56.64; H, 4.42; N, 3.84. $^{31}P\{^1H\}$ NMR: (acetone-d_6, 162.0 MHz, −80 °C): δ 36.2 (s, PPh_3), −142.5 (sept, $^1J_{PF}$ = 708 Hz, PF_6).

Separation and Single-Crystal Breeding of the Diastereomer (S_{Ru},S_C,P_{PPh_3})-[(η^6-C_6H_6)Ru(LL*)(PPh_3)]PF_6 (2a). From the mother liquor of the separation of the diastereomer (R_{Ru},S_C,P_{PPh_3})-[(η^6-C_6H_6)Ru(LL*)(PPh_3)]PF_6 (**2b**; see below), the remaining diastereomer mixture was precipitated quantitatively by slow addition of petroleum ether with stirring. The dry, microcrystalline residue was dissolved in 7 mL of acetone and 14 mL of methanol. Then, 10 mL of water was added. After 2 days of standing at 5 °C, 1.4 mL of water was added. Further standing for 1 day at 5 °C completed the precipitation. The dried precipitate was dissolved in 4.4 mL of CH_2Cl_2. Addition of 3.6 mL of *n*-hexane resulted in the formation of crystals after about 1 h. After 3 days, prismatic crystals suitable for X-ray analysis were isolated by decantation and washed with CH_2Cl_2/petroleum ether (1:3) and petroleum ether. ^{1}H NMR spectroscopy at room temperature showed only the signals of the diastereomer **2a** with the high-field singlet at 5.68 ppm for the η^6-benzene ligand (Table 1). Yield: 180 mg (0.23 mmol, 51% with respect to the **2a** content before crystallization). Mp: >250 °C dec. Anal. Calcd for $C_{37}H_{34}F_6N_2P_6Ru$: C, 56.71; H, 4.37; N, 3.58. Found: C, 56.44; H, 4.50; N, 3.75. $^{31}P\{^1H\}$ NMR (acetone-d_6, 162.0 MHz, −80 °C): δ 40.2 (s, PPh_3), −142.5 (sept, $^1J_{PF}$ = 708 Hz, PF_6).

X-ray Crystallography. The details of the crystal structure determinations are summarized in Table 4. All structures were solved using a combination of Patterson−Fourier and least-squares methods.

Data Collection for Complexes 1a, 2a, and 2b. Cell constants for the three complexes were obtained from least-squares refinement of the setting angles of 28, 25, and 15 centered reflections in the ranges 4.0° < 2θ < 25.0°, 10.0° < 2θ < 24.0°, and 4.0° < 2θ < 18.0°, respectively. The data were collected in the ω-scan mode, and in all cases 3 standard reflections were measured every 100 reflections. No profound loss of intensity was observed in the case of complexes **1a** and **2a**. For complex **2b**, the reflex intensities decreased relatively quickly (see structure solution). In all cases the data were corrected for Lorentz and polarization factors.

Structure Solution and Data Refinement for Complexes 1a and 2a. The absolute configurations were determined by refinement of Rogers' least-squares variable η (=1.1(1) for **1a** and 1.0(2) for **2a**, which confirms the S_{Ru},R_C configuration in both cases).[42,43] In the case of **1a** the Friedel pairs were measured in the 2θ range 3.0−47.5°. Because of the relatively low number of reflections in the case of complex **2a**, a refinement in three blocks was chosen (see Table 4, footnote *c*). The eight phenyl substituents of the two independent cations in the unit cell of the crystal of **2a** were refined isotropically as regular hexagons. Hydrogen atoms were added in calculated positions with the option HFIX of the SHELXTL PLUS program package.[43] They were included in structure factor calculations but were not refined. Neutral atom scattering factors were used in both cases.[44]

Structure Solution and Data Refinement for Complex 2b. The refinement of Rogers' least-squares variable η for the R_{Ru},S_C configuration seen in Figure 4 gave a value of 1.0(7).[42,43] The reflex intensities decreased very quickly due to the extreme thinness of the measured crystal. This was the reason for the isotropic refinement of the four phenyl substituents; the η^6-benzene group was also refined isotropically due to possible nonrigidity in the solid state or positional disorder. The remainder of the procedure was carried out as described above for complexes **1a** and **2a**.

Acknowledgment. We thank the Deutsche Forschungsgemeinschaft, the Fonds der Chemischen Industrie, and BASF AG, Ludwigshafen, Germany, for support of this work.

Supporting Information Available: Tables of atomic coordinates and equivalent isotropic displacement parameters, bond lengths, bond angles, anisotropic displacement parameters, and H atom coordinates and isotropic displacement parameters for (S_{Ru},S_C)-[(η^6-C_6H_6)Ru(LL*)Cl] (**1a**), (S_{Ru},S_C,P_{PPh_3})-[(η^6-C_6H_6)Ru(LL*)(PPh_3)]PF_6 (**2a**), and (R_{Ru},S_C,P_{PPh_3})-[(η^6-C_6H_6)Ru(LL*)(PPh_3)]PF_6 (**2b**) (21 pages). Ordering information is given on any current masthead page. Further details of the structure determination have been deposited with the number CSD-59180 at the Fachinformationszentrum Karlsruhe, Gesellschaft für wissenschaftlich-technische Information mbH, D-76344 Eggenstein-Leopoldshafen 2, Federal Republic of Germany.

OM960215A

(42) Rogers, D. *Acta Crystallogr.* **1981**, *A37*, 734.
(43) Sheldrick, G. M. SHELXTL PLUS, A Program for Crystal Structure Determination, release 4.11/V; Siemens Analytical X-Ray Instruments, Madison, WI, 1990.
(44) *International Tables for X-Ray Crystallography*; Kynoch Press: Birmingham, U.K., 1974; Vol. IV.